Journal of Alloys and Compounds 509 (2011) L279–L283

Contents lists available at ScienceDirect

Journal of Alloys and Compounds

journal homepage: www.elsevier.com/locate/jallcom

Letter

Fabrication of SiC particulate reinforced AZ91D composite by vacuum-assisted pressure infiltration technology

Bowen Xiong[a,b,*], Huan Yu[a,b], Zhifeng Xu[a,b], Qingsong Yan[a,b], Changchun Cai[a,b]

[a] National Defence Key Discipline Laboratory of Light Alloy Processing Science and Technology, Nanchang Hangkong University, Nanchang 330063, PR China
[b] School of Aeronautical Manufacturing Engineering, Nanchang Hangkong University, Nanchang 330063, PR China

ARTICLE INFO

Article history:
Received 6 April 2011
Received in revised form 25 April 2011
Accepted 28 April 2011
Available online 10 May 2011

Keywords:
Metal matrix composites
Microstructure
CTE
Pressure infiltration

ABSTRACT

The AZ91D Mg matrix composites reinforced by SiC particulate with the sizes of 11 μm, 21 μm and 47 μm were successfully fabricated respectively by vacuum-assisted pressure infiltration technology. Microstructures and particulate distributions were analyzed with scanning electron microscope (SEM), X-ray diffraction (XRD) and transmission electron microscope (TEM). The coefficient of thermal expansion (CTE) measurements was performed from 75 °C to 400 °C at a heating rate of 5 °C/min. The results show that the uniform distribution of SiC particulate in metal matrix and density over 98% in theoretical density of composites were fabricated. Only MgO phase was detected at the interface and no brittle phases of Al_4C_3 and Mg_2Si were discovered. The desirable coefficients of thermal expansion of composites were achieved. The intensity of dislocation generation nearby SiC particulate increases significantly with the increasing of SiC particulate size. Therefore, this technology is a potential method to fabricate Mg matrix composites reinforced by SiC particulates with the desirable microstructures and CTE.

1. Introduction

High volume fraction SiC particle reinforced light metal matrix composites have attracted much attention in multifunctional electronic packaging due to low thermal expansion coefficient [1,2]. On the other hand, the high volume fraction SiC particle reinforced light metal matrix composites show a high potential for structural applications in sectors where low weight, high stiffness and strength as well as low thermal distortion are required, such as in sporting, automotive engineering, aerospace industry, high accuracy mechanical engineering or defense technology [3,4]. Magnesium alloys are the lightest metallic structure materials having highest special strength [5]. Therefore, the high volume fraction SiC particle reinforced magnesium alloys matrix composites have attracted a lot of interest because of their attractive properties, such as a low density, a high specific strength, stiffness and coefficient of thermal expansion [3,6]. However, the studies on the fabrication of High volume fraction SiC particle reinforced Mg matrix composites are still limited compared to that of Al matrix composites.

Among all the techniques available for processing of metal matrix composites (MMCs), pressure infiltration of molten metals into porous ceramics performs is the technique suitable for fabricating the net shape and high volume fraction (>50 vol.%) MMCs [7,8]. The fabrication temperature and production time of the MMCs in the pressureless/pressure infiltration method are the higher and longer than those of other fabrication methods, which may cause severe interfacial reactions. Some interfacial reactions in metal matrix composites can effectively improve the mechanical properties of composites by enhancing of the wettability between particulates and molten metal [9–12], but some of interfacial reactions also cause the degradation of mechanical properties due to the formation of brittle and unstable phases (e.g., Al_4C_3).

Therefore, the aim of the present study is to achieve desirable interface quality in composites by coupling vacuum technology with pressure infiltration method for the decreasing of infiltration temperature and contact time between SiC and Mg to fabricate high volume fraction SiC particle reinforced magnesium alloys matrix composites, and to study the microstructures and CTE of as-cast composites.

2. Experimental procedure

The green and abrasive grade SiC particles (11 μm, 21 μm and 47 μm) with a purity of 98.5% were used respectively in this study. The AZ91D Mg alloy was employed and the chemical composition was given in Table 1. The SiC particles were natural stacked into a ceramic tube with the diameter of 20 mm, subsequently the AZ91D Mg alloy ingot was also stuffed into ceramic tube above the SiC particles. The ceramic tube was placed in an electric resistance furnace kept in closed device. Before the heating of Mg alloy, the closed device was vacuumized to about 1 kPa. When the temperature of Mg alloy was raised to 670 °C and held for 10 min,

* Corresponding author at: National Defence Key Discipline Laboratory of Light Alloy Processing Science and Technology, Nanchang Hangkong University, Nanchang 330063, PR China. Tel.: +86 791 395 3300; fax: +86 791 3953 300.
E-mail address: bowenxiong@163.com (B. Xiong).

0925-8388/$ – see front matter. Crown Copyright © 2011 Published by Elsevier B.V. All rights reserved.
doi:10.1016/j.jallcom.2011.04.136

Table 1
Chemical compositions of AZ91D Mg alloy (wt.%).

Material	Al	Zn	Mn	Si	Fe	Cu	Be	Ni	Mg
AZ91D	8.94	0.70	0.19	0.02	0.001	0.002	0.006	0.007	Bal.

a gas pressure of 400 kPa was added and held for 30 s for the infiltration of molten Mg into SiC particles, and subsequently the composites were air-cooled to room temperature.

Microstructure characterization specimens were prepared by grinding from 320 to 1200 grit paper and metallographically polished with 1 μm alumina. The microstructure has been examined using a MeF-3 optical microscope and a JSMT-200 scanning electron microscope. D/MAX-IIIB X-ray diffraction was performed on the bulk specimens for identification of phases. JEOL 1210 transmission electron microscope was used to analyze the interfacial phases. The distribution of phase and chemical species has been analyzed using JXA-800R electron microprobe analysis.

The specimens for CTE testing with the dimension of Φ 6 mm × 20 mm were machined from the composites rods. The CTE measurements were performed from 75 °C to 400 °C at a heating rate of 5 °C/min using a Netzsch DIL402 C dilatometer. The density of the fabricated composites was measured by Archimedes' method. The volume fraction of SiC particulates is determined by Image-Pro Plus soft. Each sample was analyzed five times to determine the average value of volume fractions.

3. Results and discussion

The real SiC volume fractions of Mg matrix composites reinforced by SiC particulate with the size of 11 μm, 21 μm and 47 μm were measured respectively, and the real SiC volume fractions are 55.03 vol.%, 56.79 vol.% and 54.38 vol.% respectively. The distribution of SiC particulate reinforcement in composites is presented in Fig. 1. The SEM study of composite samples reveals uniform distribution of SiC particulate throughout the Mg matrix. The densities of composites are listed in Table 2. The composites reinforced by SiC particulate with more than 98% of theoretical density were fabricated. The XRD patterns of the composites are presented in Fig. 2. Individual phases were identified by matching the characteristic XRD peaks against JCPDS data. It is obvious from Fig. 2 that the peak of MgO phase was detected composite but the peaks of Al_4C_3 and Mg_2Si were not detected. This result shows that the brittle and unstable Al_4C_3 and Mg_2Si phases are suppressed. Therefore, the present fabrication technology is fit for the fabrication of SiC particulates reinforced AZ91D Mg matrix composites having desirable interface and uniform distribution of SiC particulate. In order to further analyze the interfacial reactions, the interfacial regions of the as-cast composites were observed by TEM and the phases were determined by the electron diffraction analysis. The typical interfacial micrographs of composites are shown in Fig. 3. The interfacial micrographs of composites are clean and no obvious reaction layer appears in Fig. 3(a). However, there is still some reaction produces occurred at interface in Fig. 3(b). This phase was identified as MgO by the selected area diffraction analysis in Fig. 4. This is in good agreement with the result of XRD.

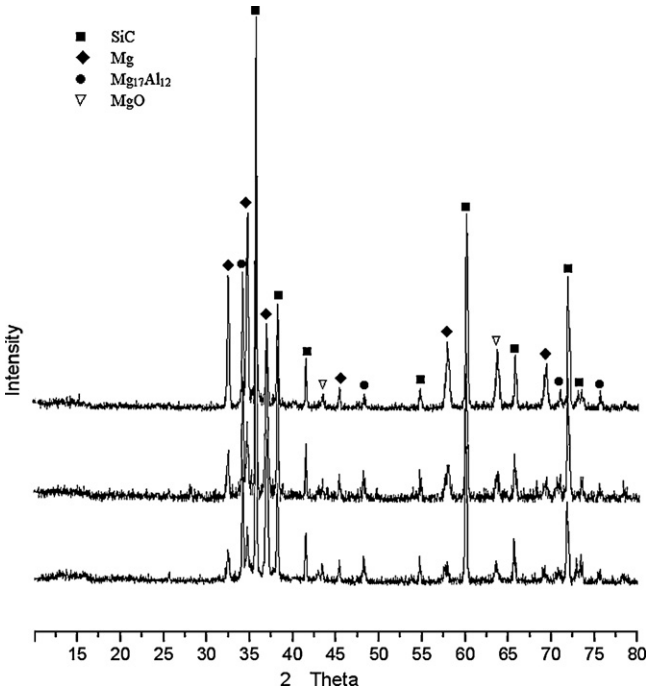

Fig. 2. XRD patterns of the composites.

The SiC/Mg–Al composite system can be thought as an Al–Mg–Si–C–O system, The presence of Al_4C_3, Mg_2Si, MgO, $MgAl_2O_4$, Al_2O_3 and Si phases formed by interfacial chemical reactions among Mg, Al, O and SiC has been reported [13], according to the following equations.

$$4Al + 3SiC \rightarrow Al_4C_3 + 3Si \quad (1)$$

$$2Mg + SiO_2 \rightarrow 2MgO + Si \quad (2)$$

$$2Al + 5Mg + 2SiO_2 \rightarrow MgAl_2O_4 + 2Mg_2Si \quad (3)$$

$$2Mg + Si \rightarrow Mg_2Si \quad (4)$$

$$4Al + 3SiO_2 \rightarrow 2Al_2O_3 + 3Si \quad (5)$$

Since the bonds in MgO, $MgAl_2O_4$, and Al_2O_3 are obviously stronger than that in Al–C, Mg–Al and Mg–Si bonds [13], oxide

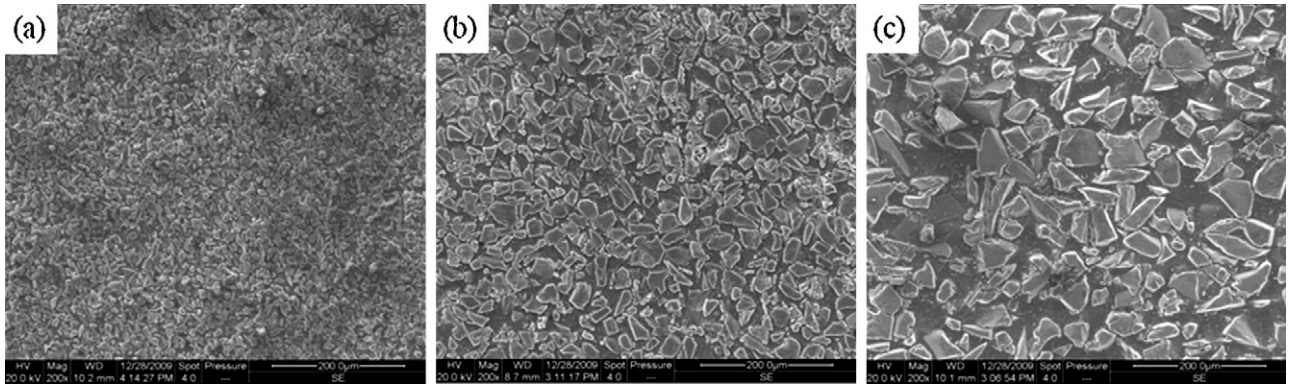

Fig. 1. Distribution of SiC particulate reinforcement in composites wih different size of SiC particulate: (a) 47 μm; (b) 21 μm; (c) 11 μm.

Table 2
Densities of composites with different SiC particulate size.

Size of SiC particulate (μm)	Theoretical density (g/cm^3)	Experimental density (g/cm^3)	Relative density (%)
11	2.580	2.549	98.81
21	2.605	2.560	98.29
47	2.571	2.515	97.83

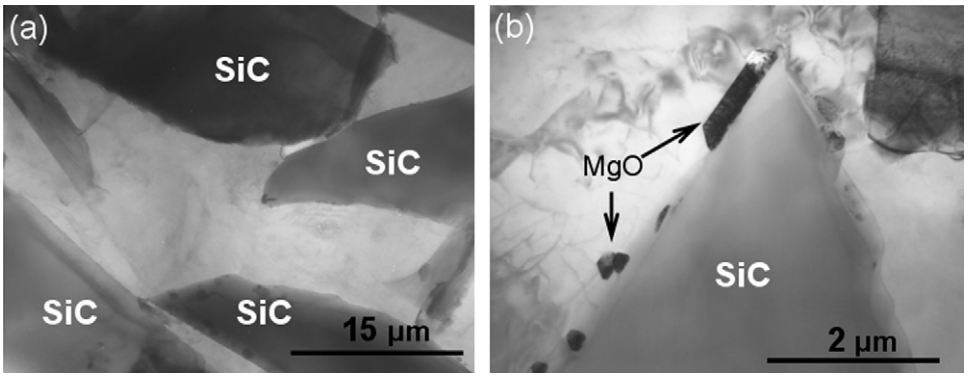

Fig. 3. Typical interfacial micrographs of composites.

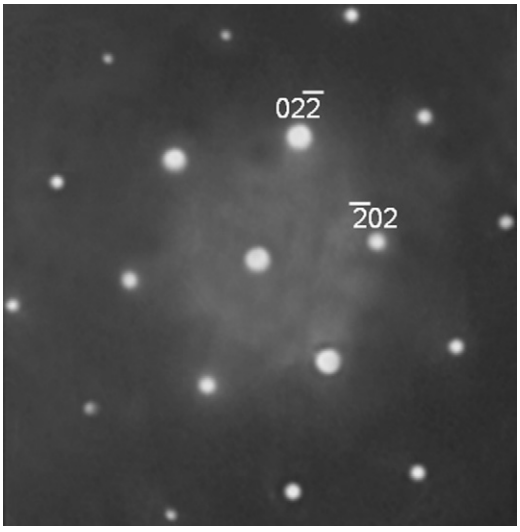

Fig. 4. Selected area diffraction analysis of MgO phase at interface.

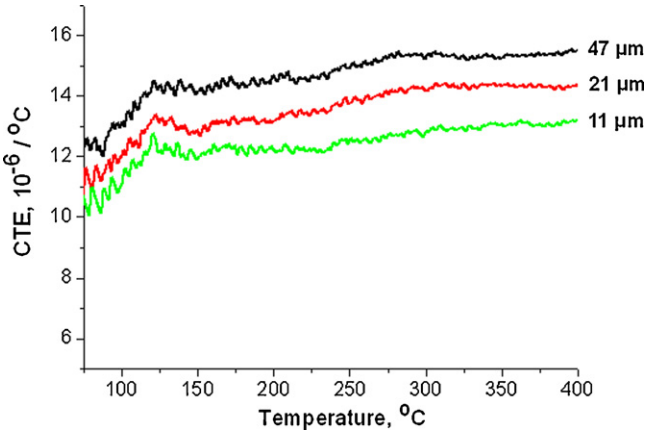

Fig. 6. Thermal expansion coefficient values as a function of temperature.

phases often form in preference to other possible compounds, for example Al_4C_3 and Mg_2Si. Among the possible oxides, the free energy for the formation of MgO is lower than that of $MgAl_2O_4$ and Al_2O_3 [14]. These thermodynamic considerations show that the most stable oxide in Mg matrix composites is MgO. Therefore, MgO phase is the most possible intermetallic compound formed during the producing procedure of these composites. On the other hands, from the analysis of composition, structure and thermodynamic theory, the desirable interfacial phase is identified as MgO.

Neither Al_4C_3 nor Mg_2Si were detected at the interface in the SiC/AZ91D composites. It indicates that the reactions (1), (3) and (4) did not take place at the interface. This phenomenon may be

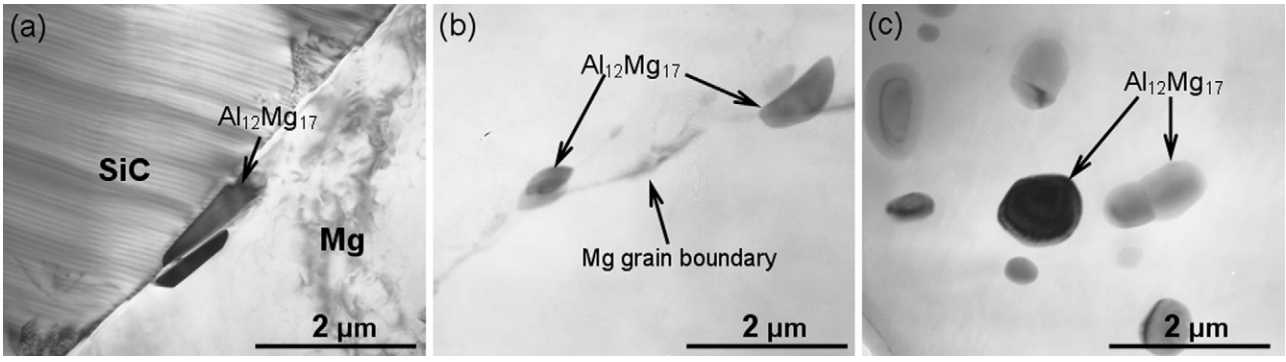

Fig. 5. Location of $Al_{12}Mg_{17}$ precipitate phases: (a) interface between SiC and Mg matrix; (b) Mg grain boundary; (c) inside Mg grain.

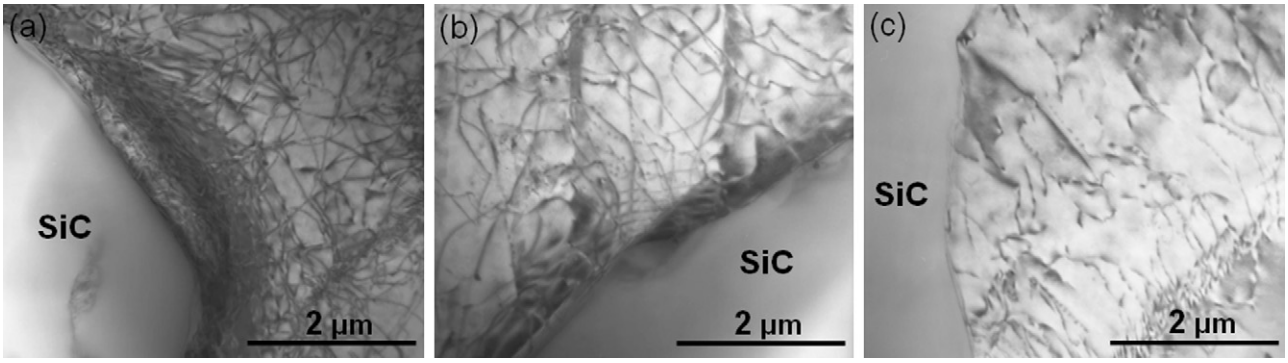

Fig. 7. Distribution of dislocation nearby SiC particulate in composites with different size of SiC particulate: (a) 47 μm; (b) 21 μm; (c) 11 μm.

explained in terms of the infiltration temperature and contact time between SiC particulate and Mg at the infiltration process. Due to the vacuum environment among SiC particulate, the flowing capacity of molten Mg among SiC particulate is significantly improved during pressure infiltration process. Therefore, the infiltration temperature and contact time between SiC particulate and Mg can be decreased for obtaining the desirable interfacial reactions. The infiltration temperature of 670 °C employed in the present study is lower than conventional infiltration temperature, resulting in the small thermodynamic driving forces for interfacial reactions. Furthermore, the contact time between SiC particulate and Mg is also short in the present study. Therefore, the interfacial reactions (1), (3) and (4) were suppressed during the pressure infiltration process.

The SiC particulate reinforced AZ91D composites samples were examined by TEM and the presence of $Al_{12}Mg_{17}$ phases were detected in the investigated microstructure in Fig. 5. When the temperature decreases to 438 °C, the eutectic reaction takes place and generates $Al_{12}Mg_{17}$ phases. The location of $Al_{12}Mg_{17}$ precipitate phases is obviously different in Fig. 5. It indicates that two different routes could be responsible for the formation of $Al_{12}Mg_{17}$ precipitate phases. The small amounts of $Al_{12}Mg_{17}$ distributed along the grain boundaries of Mg matrix and interface of SiC particulates (Fig. 5(a) and (b)) suggest that this type of $Al_{12}Mg_{17}$ precipitate phases were formed as a result of the local enrichment concentration of Al element to an exceeding concentration at the temperature in the stage of solidification of the remaining liquid, which then solidified as the (α-Mg + $Al_{12}Mg_{17}$) eutectic. The $Al_{12}Mg_{17}$ phase inside the Mg grains (Fig. 5(c)) suggests that the $Al_{12}Mg_{17}$ precipitate phases have occurred in the solid solution regions enriched with Al below the solidus temperature. This is in agreement with the results obtained by [15].

The thermal expansion coefficient values as a function of temperature for SiC particulate reinforced AZ91D composites with different particulate size were plotted in Fig. 6. It is evident that the CTE of composites increase with the increasing of SiC particulate size. This result agreed with the viewpoints obtained by Elomari [16] and Yan [17]. According to the Tayor-based nonlocal theory (TNT) of plasticity [18], the flow stress of the matrix σ_m^* in composites is given by:

$$\sigma_m^* = \sqrt{(\sigma_m)^2 + 27\sqrt{\frac{5}{2}}\beta^2\mu^2\frac{b}{a}f^{\frac{1}{3}}\varepsilon} \quad (6)$$

where σ_m is the flow stress of the matrix (AZ91D), β is an empirical constant, μ is the shear modulus of the matrix, f is the particulate volume fraction, ε is the plastic stress, b is the burgers vector, and $2a$ is the particle diameter. From Eq. (6), it can be noted the flow stress of the matrix in composites increases with decreasing the particulate size. During cooling from fabrication temperature to ambient temperature, the relaxation of the thermal stresses will be harder for composites with small particulate [17]. During reheating for CTEs testing, the higher flow stress of the matrix in the composite with the smaller particulates will restrain the plastic deformation in the matrix. Therefore, the CTEs of the composites should decrease with decreasing particulate size. The average CTEs of composites reinforced by particulate size of 47 μm and 21 μm are about 14.21×10^{-6}/°C and 13.08×10^{-6}/°C respectively, and significantly lower by 12.88% and 9.40% than that of composites fabricated by squeeze casting [19]. Therefore, the vacuum-assisted pressure infiltration technology can fabricate SiC particulate reinforced AZ91D composites with the excellent CTE. Previous literature [17,20,21] has reported that the dislocation may appear nearby SiC particulate due to the thermal mismatch. The distribution of dislocation nearby SiC particulate was given in Fig. 7. As the size of SiC particulate increases, the intensity of dislocation generation increases significantly. The dislocation density gradient was obviously observed in Fig. 7(a), but no obvious dislocation density gradient was detected in Fig. 7(b) and (c). The dislocation density is obviously related to CTE of composites, and the effects of dislocation on CTE will be detailedly considered in our future study.

4. Conclusions

The SiC particulate reinforced AZ91D composites were fabricated successfully by vacuum-assisted pressure infiltration technology. The uniform distribution of SiC particulate in metal matrix and density over 98% in theoretical density of composites were fabricated. Only MgO phase was detected at the interface and no brittle phases of Al_4C_3 and Mg_2Si were discovered. The desirable coefficient of thermal expansion of composites was achieved. The intensity of dislocation generation nearby SiC particulate increases significantly with the increasing of SiC particulate size. So, this technology is a potential method to fabricate AZ91D Mg matrix composites reinforced by SiC particulates with the desirable microstructures and CTE.

Acknowledgements

This research was financially supported by Open Foundation of National Defence Key Discipline Laboratory of Light Alloy Processing Science and Technology (GF201001003), and Aeronautical Science Foundation of China (2008ZF56016).

References

[1] G.M. Byung, S.L. Dong, S.D. Park, Mater. Chem. Phys. 72 (2001) 42–47.
[2] J.M. Molina, E. Pinero, J. Narciso, Curr. Opin. Solid State Mater. Sci. 9 (2005) 202–210.
[3] P. Poddar, V.C. Srivastava, P.K. De, K.L. Sahoo, Mater. Sci. Eng. A 460–461 (2007) 357–364.

[4] M.Y. Zheng), K. Wu, C.Y. Yao, Mater. Lett. 47 (2001) 118–124.
[5] K.K. Deng, K. Wu, Y.W. Wu, K.B. Nie, M.Y. Zheng, J. Alloys Compd. 504 (2010) 542–547.
[6] W. Li, Z. Chen, D. Chen, C. Fan, C. Wang, J. Alloys Compd. 504S (2010) S522–S526.
[7] B.S. Rao, V. Jayaram, Acta Mater. 49 (2001) 2373–2385.
[8] S.B. Ren, X.B. He, X.H. Qu, Y. Li, J. Alloys Compd. 455 (2008) 424–431.
[9] F. Delannay, L. Froyen, A. Deruyttere, J. Mater. Sci. 22 (1987) 1–16.
[10] H. Ribes, M. Suery, G. Esperance, J.G. Legoux, Metall. Trans. A 21 (1990) 2489–2495.
[11] M.Y. Gu, Z. Mei, Y.P. Jin, Z.G. Wu, Scripta Mater. 40 (1999) 985–989.
[12] S.G. Warrier, R.Y. Lin, J. Mater. Sci. 28 (1993) 760–766.
[13] A.D. Mcleod, C.M. Gabryel, Metall. Trans. A 23 (1992) 1279–1283.
[14] M.Y. Zheng, PhD thesis, Harbin Institute of Technology, PR China, 1999.
[15] A. Bochenek, K.N. Braszczynska, Mater. Sci. Eng. A 290 (2000) 122–127.
[16] S. Elomari, R. Boukhili, S. Marchi, A. Mortensen, D.J. Lloyd, J. Mater. Sci. 32 (1997) 2131–2140.
[17] Y.W. Yan, L. Geng, J. Mater. Sci. 42 (2007) 6433–6438.
[18] H. Gao, Y. Huang, Int. J. Solids Struct. 38 (2001) 2615–2637.
[19] X. Qiu, Master degree thesis, Harbin Institute of Technology, PR China, 2006.
[20] M. Vogelsang, R.J. Arsenault, R.M. Fisher, Metall. Trans. A 17 (1986) 379–389.
[21] C.T. Kim, J.K. Lee, M.R. Plichta, Metall. Trans. A 21 (1990) 673–681.